Droplet Detachment and Satellite Bead Formation in Viscoelastic Fluids

C. Wagner,[1,*] Y. Amarouchene,[2,3] Daniel Bonn,[3,4] and J. Eggers[5]

[1]*Experimentalphysik, Universität des Saarlandes, Postfach 151150, 66041 Saarbrücken, Germany*
[2]*Centre de Physique Moléculaire Optique et Hertzienne, Université Bordeaux 1 (UMR 5798), 351 cours de la liberation, 33405 Talence, France*
[3]*Laboratoire de Physique Statistique, UMR CNRS 8550, Ecole Normale Supérieure, 24 rue Lhomond, 75231 Paris Cedex 05, France*
[4]*van der Waals-Zeeman Institute, University of Amsterdam, Valckenierstraat 65, 1018 XE Amsterdam, The Netherlands*
[5]*School of Mathematics, University of Bristol, University Walk, Bristol BS8 1TW, United Kingdom*

(Received 16 July 2004; published 14 October 2005)

The presence of a very small amount of high molecular weight polymer significantly delays the pinch-off singularity of a drop of water falling from a faucet and leads to the formation of a long-lived cylindrical filament. In this Letter, we present experiments, numerical simulations, and theory which examines the pinch-off process in the presence of polymers. The numerical simulations are found to be in good agreement with experiment. As a test case, we establish the conditions under which a small bead remains on the filament; we find that the presence of a bead is due to the asymmetry induced by the self-similar pinch off of the droplet.

DOI: 10.1103/PhysRevLett.95.164504 PACS numbers: 47.55.Dz, 47.20.Dr, 47.20.Gv, 83.80.Rs

The pinch off of liquid drops, often with viscoelastic properties, has attracted considerable attention in recent years [1], not the least owing to its enormous technological applications in biotechnology, microscale manufacturing, and spray technology [2–4]. From the fundamental side, the addition of minute amounts of polymers has been shown to inhibit the finite-time singularity that happens at breakup [5]. From the applied side, in many applications, such as fire fighting [6], ink jet printing [3], or pesticide deposition on plant leaves [7], complex fluids have been used to control or modify drop sizes. All these applications are related to the elevated elongational viscosity of polymer solutions. For dilute aqueous solutions, capillary breakup and the resulting filament thinning is the only known way to determine this crucial material parameter unambiguously in a purely elongational flow. In this Letter, we provide a complete experimental and numerical description of the first stages of drop detachment for dilute aqueous polymer solutions. A comparison between experiment and simulation enables us to quantitatively determine the polymer relaxation time and to test the model's description of the late stages of pinching.

If a drop of pure water falls from a faucet [Fig. 1(a)], the fluid neck pinches near the drop as well as near the nozzle, to also form a much smaller ''satellite'' drop. If a small amount of polyethylenoxide (PEO) is added [Fig. 1(b)], pinching is inhibited and thin cylindrical threads remain, connecting to the small satellite bead in the middle. For small nozzle radii R [cf. Fig. 1(c)], no satellite bead is formed and the thread connecting to the falling drop is uniform. All times are given relative to the time t_c when the thread is first formed. The uniform thread connected to the falling drop forms a single unit of the periodic ''beads-on-string'' structure [8,9] observed for the breakup of a polymeric jet. The satellite drop of Fig. 1(b) is a small secondary structure, typical for low-viscosity solvents [10,11].

Our experiments were performed with aqueous solutions of PEO with a molecular weight of 4×10^6 amu, in concentrations of 5 to 2000 ppm. Nozzle radii R ranged from $R = 0.25$ mm to $R = 5$ mm and the droplets were generated using a syringe pump in a quasistatic mode. Pictures

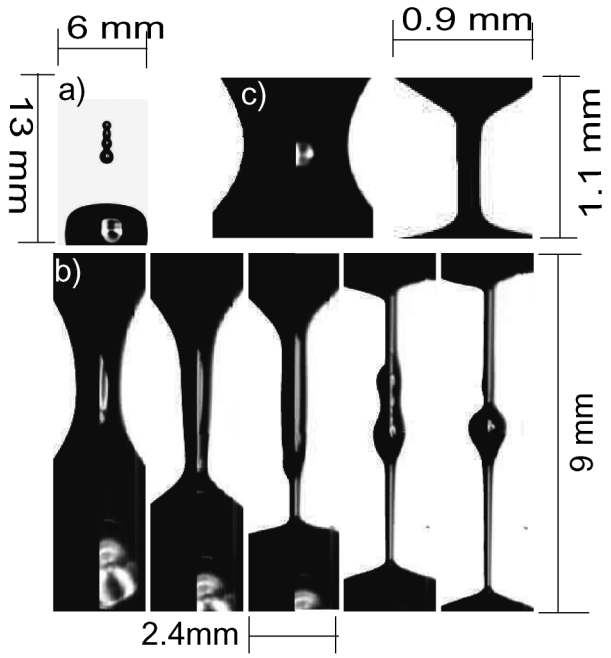

FIG. 1. (a) A drop of water falling from a faucet, the satellite drop is about to disintegrate into a number of even smaller droplets, $R = 3$ mm. (b),(c) Close-up of the pinch region, with 100 ppm of PEO solution added. Left-hand part of the photographs: numerical simulations. Right-hand part (in gray with white spots due to lensing): experiment. (b) $R = 3$ mm, $t_c - t = 6, 2, 0, -3, -5$ ms; (c) $R = 0.4$ mm $t_c - t = 1, 0$ ms. Model parameters: $\eta_p = 3.7 \times 10^{-4}$ Pa s, $\lambda = 1.2 \times 10^{-2}$ s, $b = 2.5 \times 10^4$, $\eta_s = 1 \times 10^{-3}$ Pa s, $\gamma = 6 \times 10^{-2}$ N/m.

were taken with a high speed camera (1000 frames/s with 512×512 pixels, right-hand parts of the images in Fig. 1). All experiments were repeated with different batches of polymer, with results identical to within the resolution shown.

The left-hand part of Figs. 1(b) and 1(c) are simulations of the hydrodynamic equations, describing the polymer using a FENE-P model [12], which treats a polymer as two particles connected by an entropic Hookean spring of finite extensibility. The particles are subject to viscous drag and thermal fluctuations; the spring is characterized by a relaxation time λ and a normalized maximum extensibility b. To further simplify the description, we use a 1D long-wavelength theory for the fluid motion [1], leading to a coupled set of equations for the local radius $h(z, t)$ of the fluid column, the mean fluid velocity $v(z, t)$, and the radial and axial components of the polymeric stress $\sigma_r(z, t)$, $\sigma_z(z, t)$:

$$\partial_t h^2 + \partial_z(h^2 v) = 0, \tag{1}$$

$$\rho(\partial_t v + v\partial_z v) = -\gamma\partial_z(1/R_1 + 1/R_2) + \partial_z[(\sigma_z - \sigma_r + 3\eta_s\partial_z v)h^2]/h^2 + g, \tag{2}$$

$$\partial_t\sigma_z + v\partial_z\sigma_z = [2\partial_z v + (\partial_t Z + v\partial_z Z)/Z] \times (\sigma_z + \eta_p/\lambda) - Z\sigma_z/\lambda, \tag{3}$$

$$\partial_t\sigma_r + v\partial_z\sigma_r = [-\partial_z v + (\partial_t Z + v\partial_z Z)/Z] \times (\sigma_r + \eta_p/\lambda) - Z\sigma_r/\lambda. \tag{4}$$

Equation (1) expresses volume conservation; (2) is Newton's equation for the acceleration of a fluid particle, driven by the surface tension γ times gradients of the mean curvature [first term on the right-hand side of (2)]. The second term represents polymeric stresses and viscous stresses from the solvent fluid (η_s solvent viscosity), and the final term comes from gravity. Equation (3) describes the stretching of polymers by the extensional flow $\partial_z v > 0$ inside the fluid neck, leading to the growth of axial polymer stress σ_z, while σ_r is inconsequential for the present problem. If $2\partial_z v$ is greater than the inverse relaxation time $1/\lambda$, σ_z grows exponentially until the second term of $Z = 1 + \lambda(\sigma_z + 2\sigma_r)/(b\eta_p)$ is no longer negligible, signaling full extension of the polymer chains. The zero shear rate viscosity η_p is determined by rheological measurements [13].

On the other hand, the polymer time scale $\lambda = 1.2 \times 10^{-2}$ s, needed to achieve the very good agreement between theory and experiment reported in Fig. 1, is about 4 times as large as determined by rheological measurements in [13]. Similar discrepancies have already been reported in [14] and may result from either polydispersity or multiple time scales present in a single polymer chain. The value of the extensibility parameter $b = 2.5 \times 10^4$, on the other hand, only affects the final thinning of threads, to which we return below. Again, this value is significantly higher than the value of $b = 10^4$ [13] found by rheological measurements, in line with similar discrepancies found in previous studies [14,15].

We now turn to the physical mechanism responsible for the formation of the satellite bead. From both experiment and simulation we find that the initial motion of the liquid column is well described by Rayleigh's linear theory [1,16,17], which predicts exponential growth of the most unstable mode. Thus a symmetric trough forms on the liquid bridge that separates the falling drop from the nozzle [first panel of Figs. 1(b) and 1(c)]. In the second panel of Fig. 1(b), the neck shape has turned asymmetric, signaling the transition to a nonlinear similarity solution, discussed in more detail below. For the smaller nozzle [cf. Fig. 1(c)], on the other hand, the shape turns directly to a uniform cylinder. The remaining frames of Fig. 1(b) show how the asymmetric neck structure evolves into a satellite bead.

Thus the existence of a satellite bead depends on the time at which a polymeric thread is formed: if the thread appears *before* the neck has turned asymmetric, no satellite bead is formed, otherwise there will be a satellite. Figure 2(a) shows a phase diagram for the existence of a satellite bead. For low polymer concentrations and large nozzle radius a bead is observed, while in the opposite corner, below the solid line, no bead is formed. In the narrow strip between the dashed and the solid lines a bead is formed, but it is so small that it gets stretched out by elastic stresses and eventually disappears.

To show that the condition for bead formation is given in terms of the symmetry of the initial necking alone, we use the asymmetry parameter α introduced in [17], whose value is zero for a symmetric and unity for a staircase profile. In Fig. 2(b) we show α as a function of R (at constant polymer concentration of 100 ppm), evaluated just before a thread is formed. The asymmetry parameter transitions from zero (signaling symmetric pinching) to a nonzero value at a nozzle radius which corresponds to the boundary between the ''bead'' and ''no bead'' region of the phase diagram. Plots at other polymer concentrations show similar agreement. We now derive a *quantitative* criterion for the appearance of a satellite bead. At early times Rayleigh's theory predicts growth of the disturbance of the liquid column with a rate $\omega_R = [0.118\gamma/(\rho R^3)]^{1/2}$, with γ the surface tension and ρ the liquid density. In spite of the presence of gravity, the neck profile is symmetric around its minimum radius and fits to the smallest neck diameter $h_{\min}$ (dashed lines in Fig. 3) agree remarkably well with theory (see inset), in agreement with previous work on dripping [16,17]. For later times, as the bridge becomes more strongly deformed, the *asymmetric* pinch-off solution [18] $h_{\min} = a[\gamma(t_0 - t)^2/\rho]^{1/3}$ takes over (straight lines). Here t_0 is the extrapolated singularity time, at which the droplet would pinch off in the absence of polymer. The experiments confirm the universality of the amplitude $a = 0.8$, which agrees well with the theo-

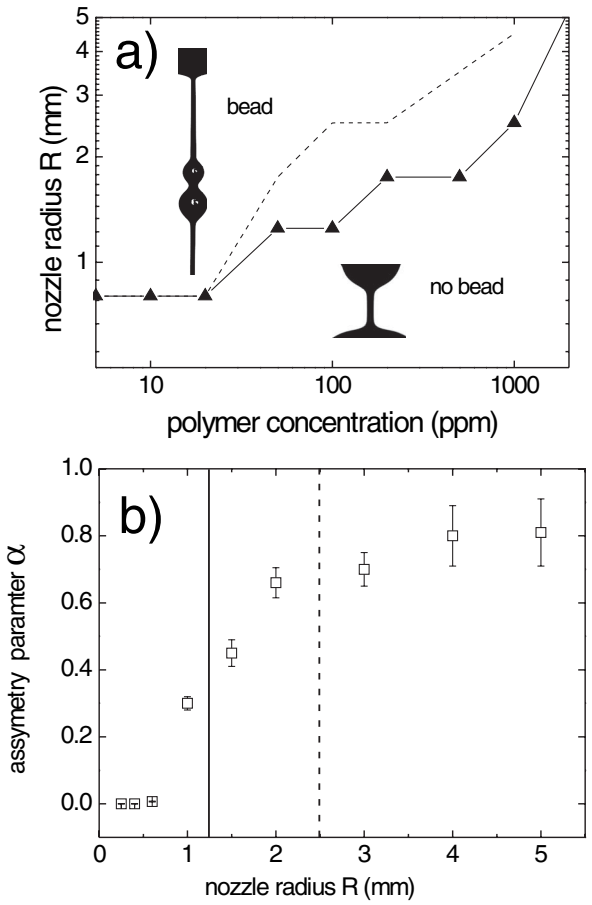

FIG. 2. (a) The phase boundary for satellite bead formation, from experimental runs at polymer concentrations of 5, 10, 20, 50, 100, 200, 500, 1000, and 2000 ppm and nozzle radii $R =$ 0.25, 0.75, 1, 1.5, 2, 3, 4, and 5 mm (triangles). Between the dashed and the solid lines a bead is formed, but subsequently disappears. (b) The asymmetry parameter α for the 100 ppm runs measured from the last video frame before the appearance of a thread. The vertical lines correspond to the transition lines in (a).

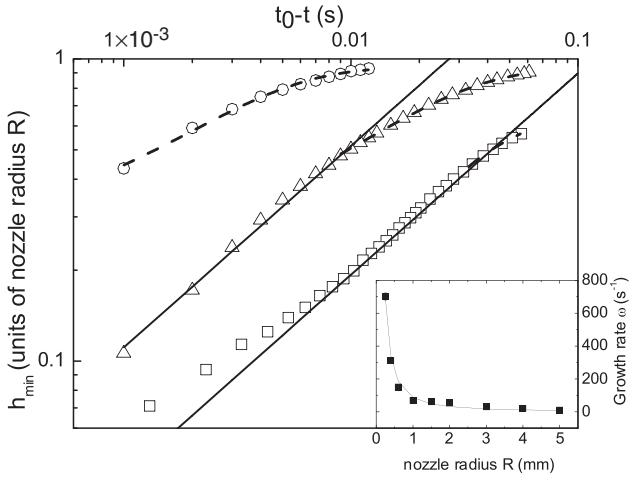

FIG. 3. The minimum neck radius versus time for nozzle radii $R = 0.4$ mm (circles), $R = 1.5$ mm (triangles), and $R = 4$ mm (squares), at a polymer concentration of 100 ppm, where t_0 is the extrapolated time at which pinch off would take place for a Newtonian liquid. The straight lines are fits to a 2/3 power law, yielding a universal prefactor of 0.8 (note that the neck radius is reported in units of R). The dashed lines are exponential fits to the disturbance amplitude $1 - h_{\min}/R$. The squares in the inset are the corresponding growth rates; the line is the theoretical prediction for the most unstable Rayleigh mode of an inviscid fluid.

retical value of $a = 0.7$ [18], considering the limited scaling range. This confirms the purely inviscid character of this stage of motion. Our observations show that the transition from an asymmetric to a symmetric shape occurs at a fixed value of $h_{\min}/R = 0.17 \pm 0.01$, corresponding to a sufficiently strong deformation of the liquid bridge. The power-law behavior of $h_{\min}$ is not observed for the smallest nozzle radius: we have not yet transited into the similarity solution regime before the elastic forces due to the polymer intervene and lead to the formation of the filament. If the growth rate ω_R of the Rayleigh instability exceeds λ^{-1}, such that polymer stretching takes place during the initial motion, no bead is formed. Thus $R_{\text{crit}} = (0.118\lambda^2\gamma/\rho)^{1/3} \approx 1$ mm is the critical radius above which a bead is formed, in good agreement with the findings for low polymer concentrations. The influence of polymer concentration is relatively minor, in agreement with this argument: the critical radius changes only by a factor of *2*, while the concentration varies by 2 orders of magnitude. The slight increase of R_{crit} with concentration reflects an increase in the relaxation time λ, due to overlap above the critical concentration $c^* = 300$ ppm [5,19].

Having obtained a reliable estimate of the FENE-P parameter $\lambda = 0.012$ s at a polymer concentration of 100 ppm from the early stages of pinching, we now turn to the description of the polymeric thread at later times. Disregarding the finite extensibility of the polymers, the thread radius is predicted [9,11] to thin as $h_{\text{thread}} = h_0 \exp[-t/(3\tau)]$, a law well supported [20] by experiments at large solvent viscosity, where $\tau = \lambda$. In the present experiment, we find exponential behavior for about a decade in radius, but the decay rate depends significantly on both the nozzle radius and the polymer concentration, in agreement with other recent experiments [19]. At a polymer concentration of 100 ppm, we find values between $\tau =$ 0.011 s ($R = 5$ mm) and $\tau = 0.003$ s ($R = 0.4$ mm). The value for the largest radius agrees with the polymer relaxation time obtained from the simulation. As we shall see below, nonlinear saturation effects are more important for small R, which is a possible reason for the smaller effective relaxation time.

Indeed, the following estimate shows that polymers have to be stretched very significantly before they generate a stress sufficient for thread formation. The total deformation the polymers have to undergo before elastic stresses become strong enough to balance surface tension can be estimated as $(R/h_{\text{thread}})^4 = [2\lambda\gamma/(\eta_p R)]^{4/3}$ [9,11].

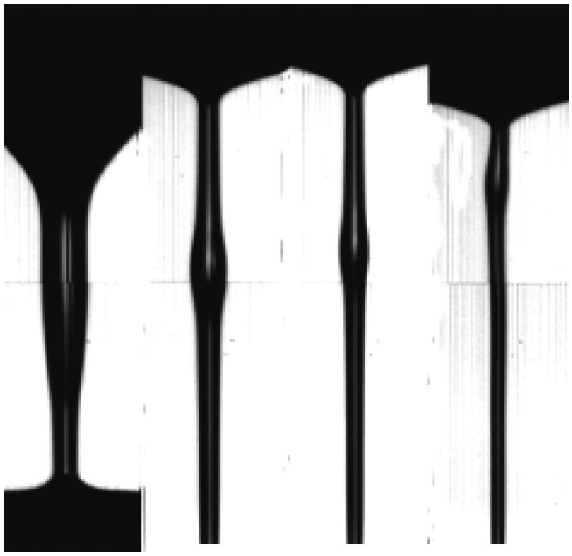

FIG. 4. The migration of the primary bead for the 50 ppm, $R = 1.5$ mm run (pictures are 1×4 mm). The profiles are shown in time steps of 2 ms. The bead is pushed upward against the direction of gravity.

Evaluating this for $R = 3$ mm, we find that the polymeric stress has increased by 1.4×10^4 at the time a thread is first formed. The rheological data of [13] suggests that at that point polymers have already reached a significant fraction of their total length, a picture that is supported within our FENE-P modeling. However, even if the thinning rates are found to be in good agreement with the experimental data in the beginning, a proper exponential thinning regime is never observed in the simulations. A significant further increase in b will eventually lead to exponential thinning, but lack of numerical resolution prevented us from exploring this regime further. When the polymeric thread has thinned to about 10 μm, it becomes yet again unstable to form tertiary beads of corresponding size. At present there is little understanding of this ''blistering'' [21,22] (too small to be visible on the scale of Fig. 1). As long as the polymers can still stretch, extensional viscosity will stabilize the thread, so the blistering instability is likely associated with the polymeric stress having reached saturation, or failure of polymer strands.

It is also worth examining the subsequent evolution of satellite beads, which can be quite varied. At least three of the scenarios predicted previously by Li and Fontelos [10] could be observed in our experiments: the disappearance of a bead due to stretching; bead migration and fusion of threads due to differences in the capillary pressure. Bead stretching (between the dashed and solid lines in Fig. 2) occurs if the bead is small and the pressure difference between the bead and the surrounding filament is small. Bead migration usually follows gravity, but smaller beads may be driven upward by pressure forces (cf. Fig. 4), where they fuse with the upper reservoir. Small beads also get sucked into larger ones [cf. Fig. 1(b)], because their internal pressure is higher.

In conclusion, we have measured and described the formation of a secondary bead during the detachment of a drop of viscoelastic liquid. The conditions for secondary bead formation are well explained by comparing time scales of the inviscid fluid motion with the time scale of the polymer, furnishing a simple method to determine model parameters relevant for large polymer deformations. Our numerical simulations describe the drop formation process in very favorable agreement with the experiments, if the polymer time scale is adjusted. Disagreement between model parameters thus obtained and rheological measurements highlight the significant challenges remaining in the quest for simple and universal dynamical models of polymeric fluids.

*Electronic address: c.wagner@mx.uni-saarland.de

[1] For a review, see J. Eggers, Rev. Mod. Phys. **69**, 865 (1997).
[2] D. B. Wallace, in Proceedings of the ''Hot Topics'' Workshop: Analysis and Modeling of Industrial Jetting Processes (http://www.ima.umn.edu/multimedia/abstract/1-10abs.html#wallace).
[3] O. A. Basaran, AIChE J. **48**, 1842 (2002).
[4] E. Villermaux, Ph. Marmottant, and J. Duplat, Phys. Rev. Lett. **92**, 074501 (2004).
[5] Y. Amarouchene, D. Bonn, J. Meunier, and H. Kellay, Phys. Rev. Lett. **86**, 3558 (2001).
[6] P. S. Virk, AIChE J. **21**, 625 (1975).
[7] V. Bergeron *et al.*, Nature (London) **405**, 772 (2000).
[8] M. Goldin, J. Yerushalmi, R. Pfeffer, and R. Shinnar, J. Fluid Mech. **38**, 689 (1969).
[9] V. M. Entov and A. L. Yarin, Fluid Dyn. **19**, 21 (1984) [Izvestiya Akademii Nauk SSSR, Mekhanika Zhidkosti Gaza **19**, 27 (1984)].
[10] J. Li and M. A. Fontelos, Phys. Fluids **15**, 922 (2003).
[11] Ch. Clasen *et al.*, cond-mat/0307611.
[12] R. B. Bird, R. C. Armstrong, and O. Hassager, *Dynamics of Polymeric Liquids* (Wiley, New York, 1987), Vols. 1–2.
[13] A. Lindner, J. Vermant, and D. Bonn, Physica (Amsterdam) **319A**, 125 (2003).
[14] R. G. Larson, *The Structure and Rheology of Complex Fluids* (Oxford University, New York, 1999).
[15] M. R. J. Verhoef *et al.*, J. Non-Newtonian Fluid Mech. **80**, 155 (1999).
[16] C. Clanet and J. C. Lasheras, J. Fluid Mech. **383**, 307 (1999).
[17] A. Rothert, R. Richter , and I. Rehberg, Phys. Rev. Lett. **87**, 084501 (2001).
[18] R. F. Day, E. J. Hinch, and J. R. Lister, Phys. Rev. Lett. **80**, 704 (1998).
[19] V. Tirtaatmadja *et al.*, Phys. Fluids (to be published).
[20] S. L. Anna and G. H. McKinley, J. Rheol. (N.Y.) **45**, 115 (2001).
[21] L. Smolka, Ph.D. thesis, Penn State University, 2002.
[22] M. S. N. Oliveira and G. H. McKinley, MIT Report No. 05-P-01, 2005.